Aluminum in complex luminescence defects in irradiated silicon

E. Irion,* N. Bürger,† K. Thonke, and R. Sauer‡
Physikalisches Institut IV, Universität Stuttgart, D-7000 Stuttgart 80, Pfaffenwaldring 57, Federal Republic of Germany
(Received 20 June 1988)

Two aluminum-related defect spectra in irradiated silicon, Al1 with a no-phonon transition at 0.836 eV and Al2 at 0.886 eV, are studied by photoluminescence measurements employing temperature control and perturbation spectroscopy with uniaxial stress and magnetic fields. Al1 is a defect of rhombic I (C_{2v}) site symmetry, probably incorporating carbon in addition to aluminum. Its optical properties are very similar to those of the Ga1 and T defects (related to Ga and C or B and C, respectively), suggesting equivalent microscopic structure of the Al1, Ga1, and T defects. For Al2, monoclinic I (C_{1h}) or trigonal (C_{3v}) symmetry is found in stress or Zeeman measurements, respectively, with annealing behavior and local modes similar to Al1.

I. INTRODUCTION

Irradiation of silicon with high-energy electrons, typically in the MeV range, and partial annealing at different temperatures creates a large number of defects that give rise to characteristic photoluminescence (PL) spectra.[1] Dominant in nominally undoped silicon are two optical defects related to the persistent, electrically inactive impurities carbon and oxygen. In oxygen-lean float-zone silicon, the spectrum with no-phonon (NP) emission at 0.97 eV ("G line") prevails; in oxygen-rich pulled silicon, the spectrum at 0.79 eV ("C line") is strongly observed in addition to the G line. Recent observation of isotope effects on the spectra which were originally reported more than 20 years ago[2,3] firmly established the role of carbon, oxygen, and silicon self-interstitials.[4–7] Microscopic models of the defects have emerged based on electron-paramagnetic-resonance measurements and related techniques consistent with the large amount of previous optical data: The 0.97-eV defect is ascribed to a C_s-Si_i-C_s complex[8] (s, substitutional; i, interstitial site) and the 0.79-eV center identified as an interstitial carbon atom trapped near an interstitial oxygen atom.[9] All other irradiation-induced luminescent defects are less well documented and understood.

The ability of the electrically active group-III and group-V impurities to form complex luminescence centers in irradiated silicon appears to be quite inequivalent. No such centers are reported in the literature in conjunction with the group-V donors. The situation for group-III acceptors is different. Boron pairs, interacting with a still unknown partner, give rise to the $I2$ line at 1.108 eV[10], and a second electronic-vibronic spectrum at 0.9351 eV ("T line") was associated with boron in addition to carbon.[11] Gallium is responsible for the defects Ga1 (0.875 eV),[12] Ga2 (1.049 eV),[13] and Ga3 (0.928 eV).[14] The latter luminescence spectra were first reported by Noonan *et al.*,[15] who also observed an aluminum-related line (Al1) at 0.836 eV. These authors mainly intended to study the influence of Al and Ga doping on the formation of the 0.97- and 0.79-eV defects, whose structure was not known at that time. With this particular intention, neither a spectrum of Al1 was exhibited nor other information advanced exceeding the annealing behavior. On the other hand, Lightowlers and Drakeford[16] observe a complex series of sharp lines in the range 1.05–1.15 eV after 450 °C thermal annealing for up to 50 h related to Al doping of the starting silicon crystals. This recent finding lends new attraction to Al as an impurity interacting with other atomic species to form pointlike optical centers.

The lack of knowledge on the initially reported Al1 defect has motivated the present investigation. Our study includes observation of a second, irradiation-dependent optical center at 0.8859 eV associated with Al as well, which we label Al2. For both spectra, we investigate annealing behavior, temperature-controlled deactivation of the luminescence, and line splittings under uniaxial stress and in magnetic fields to make symmetry assignments. Correlations with other defects are finally discussed. Experimental details are as described elsewhere.[11,12]

II. Al1 DEFECT

Our data on the growth and disappearance of the Al1 spectrum as a function of isochronal 1-h annealing steps are shown in Fig. 1 and are consistent with the result of Noonan *et al.*[15] Data sets were taken for three different samples of low-oxygen float-zone silicon at aluminum concentrations of 1×10^{15}, 5×10^{15}, and 1×10^{17} cm^{-3} with carbon and oxygen concentrations below the detection limit of 2×10^{16} cm^{-3} by ir vibrational absorption. In addition, spectra from other aluminum-doped samples, identically irradiated to a fluence of some 10^{16} electrons/cm^2, were studied in the optimum annealing stage at 300 °C. The intensity of the Al1 line is not proportional to the aluminum concentration, as some samples of significantly lower aluminum doping than others showed much stronger luminescence intensity. This indicates that aluminum needs a coactivator to form the optical defect. Other doping impurities, such as boron or phosphorus, do not appear to play a role; hence participation of oxygen or carbon would be a reasonable assumption. Noonan and co-workers[15] studied the Al1 spectrum in oxygen-rich pulled silicon and reported weak

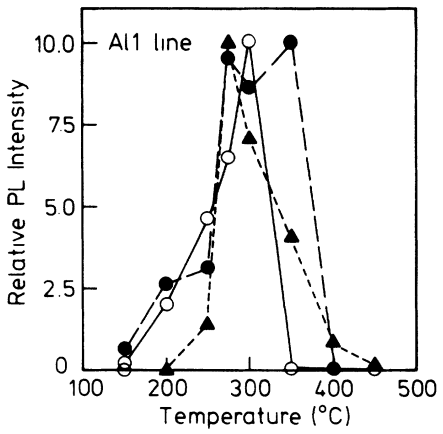

FIG. 1. Isochronal annealing (1-h steps) of the Al1 spectrum in three different samples of float-zone (FZ) silicon with Al concentrations 1×10^{15}, 5×10^{15}, and $\sim1\times10^{17}$ cm^{-3} and carbon and oxygen concentrations below 2×10^{16} cm^{-3}.

intensities of Al1 compared to the 0.97- or 0.79-eV luminescence. We also observe comparatively small signals of Al1, but in oxygen-lean float-zone silicon which tends to favor carbon as the partner of aluminum in the optical center. On the other hand, it was found[15] that Al doping inhibits formation of the 0.79-eV (C line) defect which incorporates carbon and oxygen. This would hint to either carbon or oxygen. In this study, there was no suitable ^{13}C-enriched, Al-doped silicon-crystal available to probe carbon incorporation by potential ^{13}C-^{12}C isotope shifts in the spectrum.

Figure 2 shows the Al1 electronic-vibronic photoluminescence spectrum. The NP transition at 0.8368 eV is accompanied by satellites due to lattice phonons or local vibrational modes (cf. Table I). The satellite $(Al1)^1$ shifted from the NP transition by 64.4 meV close to the energy of the O^Γ zone-center optical phonon is dominant. Due to the relative sharpness and large intensity of this satellite, we assign the line to a defect-modified O^Γ lattice mode. Other satellites are much weaker. Their positions and displacement energies from the NP transition are given in Table I with possible assignments indicated.

TABLE I. Al1 luminescence spectrum with line positions and assignments.

Line	Photon energy (meV)	Displacement from NP line (meV)	Remarks
$(Al1)^0$	836.8		NP transition
TA	819.8	17	TA replica
1	804.9	31.9	2×TA
2	796.6	40.2	LA (?)
3	777.6	59.2	TO
$(Al1)^1$	772.4	64.4	defect-modified O^Γ
4	765.1	71.7	local mode
5	759.0	77.8	
6	724.0	112.8	local mode
7	709.1	127.7	2×$(Al1)^1$

The thermal deactivation of the Al1 line is exhibited in Fig. 3. The luminescent state of the defect is stable up to $\approx$20 K and is then dissociated in two steps, suggesting thermal occupation of an intermediate excited state. Theoretical fits employing a three-level scheme yield (15±5)-meV excitation energy of the intermediate state above the luminescent ground state, and a final dissociation energy of the order of 150 meV. Excitation spectroscopy performed on the Al1 defect with a tunable color-center laser[17] yielded the TA lattice phonon as a broad

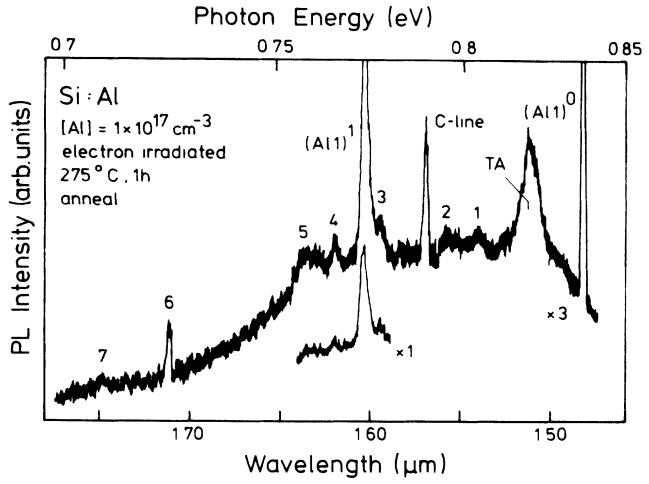

FIG. 2. Al1 spectrum with no-phonon transition $(Al1)^0$ at 0.8368 eV in an oxygen-lean, Al-doped FZ silicon sample after irradiation and annealing at 275 °C. For line positions, see Table I.

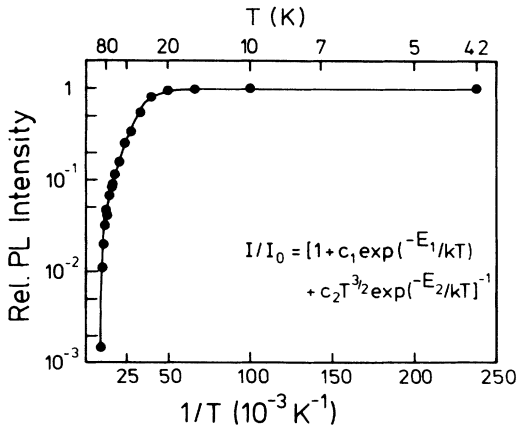

FIG. 3. Thermal deactivation of the Al1 line. Solid line is a fit (three-level scheme) with dissociation into the conduction or valence band proportional to $T^{3/2}$. The expression used is given in the figure with the parameters $E_1=14$ meV, $E_2=145$ meV, $C_1=1500$, and $C_2=2\times10^7$ K$^{-3/2}$.

anti-Stokes line and two sharp electronic lines at 21 and 28.4 meV in excess of the NP transition energy. The 21-meV state could be identical to the thermally deduced excited state at 15±5 meV.

The site symmetry of the Al1 center was determined by studying the NP line under uniaxial strain. Stress X up to 320 MPa was applied, directed along ⟨001⟩, ⟨111⟩, and ⟨110⟩ crystal axes in suitably cut samples. The splitting of the Al1 line is shown in Fig. 4, which also presents selected spectra at specific stress values with π- and σ-polarized portions of the stress-split components indicated. The relatively broad low-energy component for $\mathbf{X}\|\langle 110\rangle$ exhibits the largest splitting rate and is therefore most sensitive to stress inhomogeneities explaining the width of that line. As there is no thermalization among the various components for a given stress direction, we interpret all splittings as being due to the lifting of orientational degeneracies. The number of components and the observed prevailing polarization features are consistent with the luminescence light corresponding to a π oscillator at a defect in the rhombic I (C_{2v}) symmetry group.[18] This means that the transition is polarized parallel to the z axis of the defect. Good fits to the splitting rates in Fig. 4 can be made with the set of piezooptic constants (in units of meV/GPA,

$$A_1 = 17.5, \quad A_2 = -16.0, \quad A_3 = 23.3 ,$$

confirming the C_{2v}-symmetry assignment. Upon diagonalizing the piezooptic tensor[18] with these tensor elements one obtains eigenvalues of 17.5, 7.3, and −39.3 in the defect coordinate system $\hat{\mathbf{z}}, \hat{\mathbf{y}}, \hat{\mathbf{x}}$. The big difference of the values for $\hat{\mathbf{x}}$ and $\hat{\mathbf{y}}$ indicates that the center is "hard" toward deformation in one of the two directions but "smooth" in the other perpendicular direction. This finding is similar to the case of the Ga1 center and can be explained by an essentially planar defect configuration.

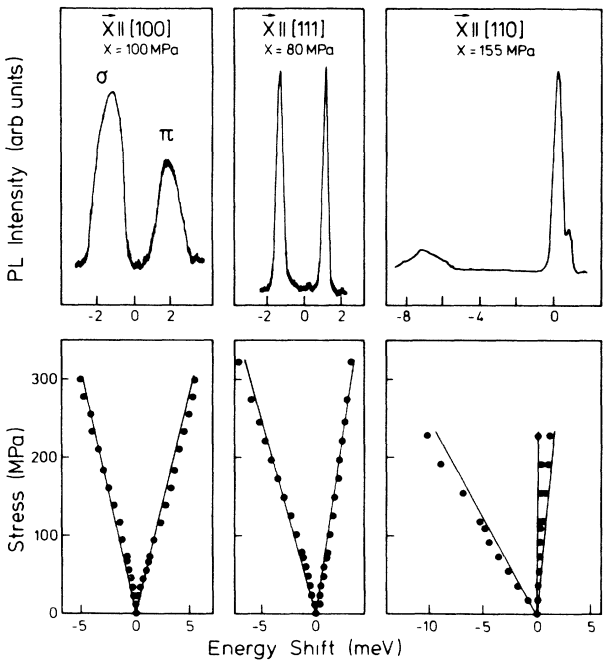

FIG. 4. Lower diagrams: splitting of the $(Al1)^0$ line when uniaxial stress is applied along ⟨001⟩, ⟨111⟩, and ⟨110⟩ crystal directions. Upper diagrams: spectra at specific stress values. Polarization of the stress split components is mixed π and σ unless otherwise indicated. Solid lines in the lower diagrams are fits employing the piezooptic constants given in the text.

In magnetic fields of 5.3 T the dominant emission is a line or "group" of lines close to the unperturbed position of the $(Al1)^0$ transition. The splitting of the "group" is very small and anisotropic, with a single line for $\mathbf{B}\|\langle 001\rangle$ and at least two components for the other directions most widely split apart for $\mathbf{B}\|\langle 111\rangle$ and less widely for $\mathbf{B}\|\langle 110\rangle$. Very weak outer components were observed for some orientations of the magnetic field, displaced from the central group by energies corresponding to g values of 1.3–1.7. Despite the limited data, the basic interpretation is evident and similar to that discussed in detail later in this paper for Al2: The Al1 line is due to an electron ($s=\frac{1}{2}$) recombining with a spinlike hole ($s=\frac{1}{2}$) whose orbital momentum is quenched. There are almost no admixtures of orbital states to the hole spin; hence the outer Zeeman transitions, $m_s(\text{electron}) = \pm\frac{1}{2} \rightarrow m_s(\text{hole}) = \mp\frac{1}{2}$, are rather strictly forbidden (cf. Figs. 8 and 9). The anisotropic fine splitting of the central emission hints to trigonal (C_{3v}) symmetry of the defect in magnetic fields. It is noteworthy that the general recombination scheme, $s=\frac{1}{2} \rightarrow s=\frac{1}{2}$, not only applies to the two present Al-related luminescence defects, but also to the Ga1 and T centers (Refs. 12 and 11, respectively).

III. Al2 DEFECT

The Al-related defect photoluminescence spectrum, with NP transition $(Al2)^0$ at 0.8859 eV, has not been reported before. It grows in close to 250 °C, peaks at around 300 °C, and is quenched close to 400 °C (Fig. 5). This annealing behavior was observed for the three samples characterized earlier in conjunction with Al1. The annealing behavior of Al2 is practically identical to that of the Al1 spectrum.

In all samples studied the Al1 spectrum was superimposed on the Al2 spectrum at much larger intensities. This hampers identification of vibronic satellites associated with the NP transition $(Al2)^0$. The weak Al2 spectrum is further obscured by the 0.79-eV C line and its sideband. Comparison of samples showing the Al1 and Al2 spectra at different relative intensities demonstrates that the line labeled $(Al2)^1$ in Fig. 6 is associated with the $(Al2)^0$ NP transition. The corresponding mode has $h\nu = 66.6$ meV and is interpreted as a defect-modified lattice vibration similar to the Al1 defect.

Temperature-controlled measurements were conducted but are relatively inaccurate due to the weakness of the spectrum. The luminescent state of the Al2 defect is stable up to ≈20 K. It is then dissociated in two steps: the first step indicating an excited upper state 7–14 meV above the luminescent state, and the second step indicating a dissociation energy of the localized electron-hole pair of very roughly 90 meV.

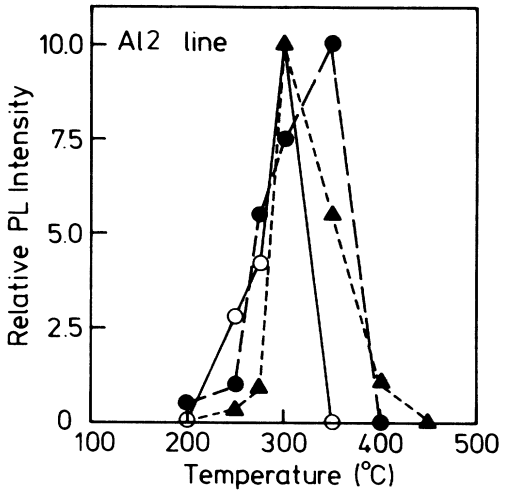

FIG. 5. Isochronal annealing (1-h steps) of the Al2 spectrum in the three samples of Fig. 1.

The effect of uniaxial stress on the $(Al2)^0$ line is shown in Fig. 7. For stress along each of the principal crystal directions, the splitting rates are nonlinear, suggesting interactions with an electronic excited state a few millivolts above the luminescent ground state. [An excited state line ≈ 3 meV above $(Al2)^0$ was indicated in higher-temperature spectra, but could not be unambiguously related to the Al2 spectrum.] The number of stress-induced components is 2, 2, and 3 for stress along $\langle 100 \rangle$, $\langle 111 \rangle$, and $\langle 110 \rangle$, respectively. This is consistent either with an E-to-A transition at a center of trigonal symmetry, including lifting of the electronic degeneracy of the

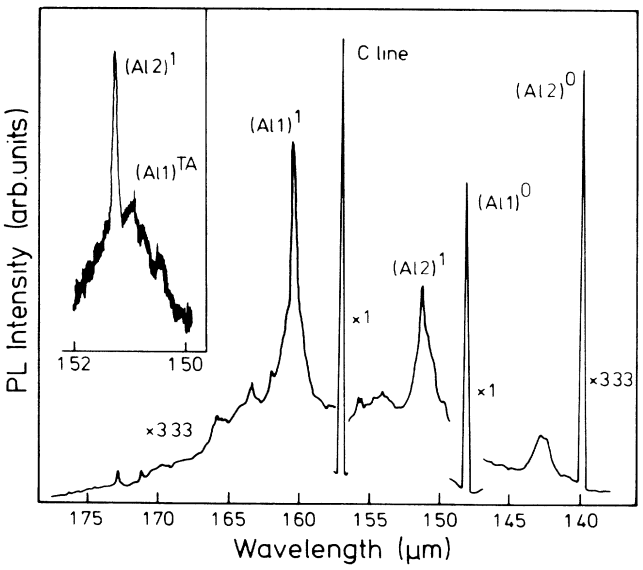

FIG. 6. Al2 spectrum showing the no-phonon transition $(Al2)^0$ at 0.8859 eV and the local-mode satellite $(Al2)^1$ at 0.8193 eV. Inset: high-resolution spectrum separating $(Al2)^1$ from the broad TA replica of $(Al1)^0$.

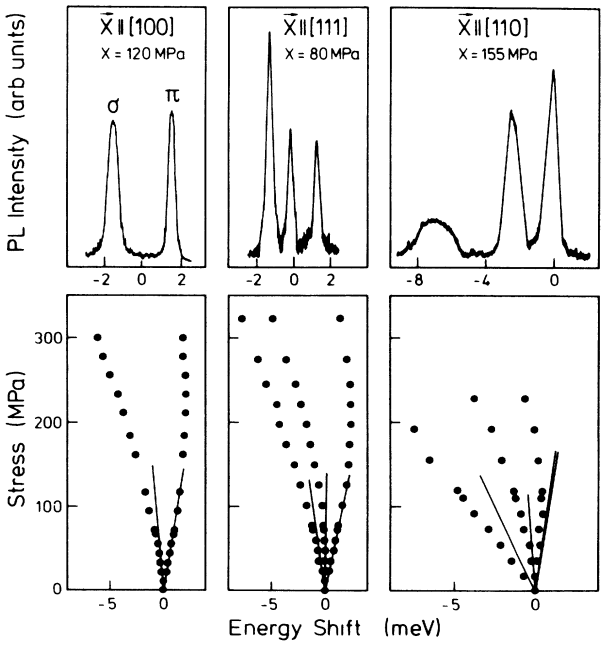

FIG. 7. Lower diagrams: splitting of the $(Al2)^0$ line under uniaxial stress directed along $\langle 001 \rangle$, $\langle 111 \rangle$, and $\langle 110 \rangle$ crystal directions. Upper diagrams: spectra at selected stress values with π or σ polarizations of the stress-split components. Fits in the lower diagrams employ the piezospectroscopic constants given in the text and refer to the linear splitting regimes at low stresses.

E-symmetric state,[18,19] or with an A-to-A transition at a center of monoclinic (C_{1h}) symmetry, where the observed splittings are all due to the lifting of the orientational degeneracy.[18,19] In either case, there must be accidental coincidence of two components for $\mathbf{X} \| \langle 110 \rangle$. As no thermalization is observed between any of the stress-induced line components and as the defect ground state is neutral (i.e., A symmetric), we assume purely orientational splittings in the C_{1h} point group. Limiting the analysis to the initial linear splitting regime at low stresses, we were able to find a set of piezooptic parameters in satisfactory agreement with the data in Fig. 7. The parameters are (in units of meV/GPa)

$$A_1 = 13.5, \quad A_2 = -8.0, \quad A_3 = -16.5, \quad |A_4| = 6.5 .$$

Corresponding calculated splitting rates are compared in Fig. 6 to the experimental data. Comparison of experimental and group-theoretical polarizations is not particularly helpful in the present case. For C_{1h} site symmetry, transitions between states transforming as the same irreducible representations are π polarized and those between states transforming as different representation are σ polarized.[20] Taking into account the twofold Kramers degeneracy under strain in the C_{1h} double group, the states are linear combinations of Γ_3 and Γ_4; hence transitions $\Gamma_3+\Gamma_4 \rightarrow \Gamma_3+\Gamma_4$ are mixed π- and σ-polarized light.

Zeeman measurements were carried through up to

magnetic fields of 5.3 T. For all field directions the Al2 line splits basically into a triplet with a dominant central component or group of lines and two weak outer components (Fig. 8). Similar basic triplet patterns have previously been reported for the luminescence lines of the Ga1 defect[12] and the T defect.[11] Adopting the interpretation from these cases we ascribe the present triplet to the recombination of an $s=\frac{1}{2}$ electron with a weakly interacting spinlike $s=\frac{1}{2}$ hole whose orbital momentum is quenched. Remaining orbital admixtures to the spin states render the $m_s=\pm\frac{1}{2}\rightarrow\mp\frac{1}{2}$ transitions weakly allowed (Fig. 8). Quenching of the hole orbit implies that the hole is tightly bound experiencing the true site symmetry of the defect. This gives rise to the anisotropic fine splittings observed in the angular dependence of the Zeeman spectra (Fig. 9). Within the model they can be fitted assuming trigonal (C_{3v}) defect symmetry with g_e(isotropic)$=2$ for the electron and $g_{\parallel}=3.2$ and $g_{\perp}=1.6$ for the hole, yielding an effective value of $g_h=\frac{1}{3}(g_{\parallel}+2g_{\perp})=2.1$ In Fig. 9 the difference between the experimental data points and the fit in the high-energy branch is outside the experimental error. These deviations are similar to the Zeeman data of the T line,[11] and as in that case could indicate interactions with a low-lying excited state. The discrepancy between the trigonal or monoclinic symmetry assignments from Zeeman or stress data, respectively, can be reconciled. We assume that only the heavy perturbation by the applied stress pins the defect in a static C_{1h} configuration corresponding to its true site symmetry, whereas dynamic averaging between the three equivalent C_{1h}-symmetric configurations around a ⟨111⟩ axis leads to the trigonal symmetry observed under the weak Zeeman perturbation. Such behavior was convincingly demonstrated for the 0.97-eV defect in optically detected magnetic resonance measurements[8] and occurred for temperatures in excess of ≈ 15 K. This explanation is also plausible in the present case as diagonalization of the piezooptic tensor[18] yields one of the principal axes of the defect in a (110) plane 2° from a ⟨111⟩ direction.

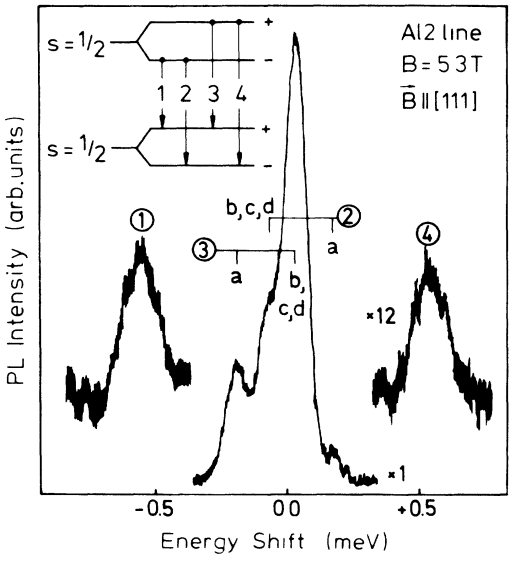

FIG. 8. Zeeman spectrum of the (Al2)^0 line for $\mathbf{B}\parallel[111]$. Inset shows basic $s=\frac{1}{2}$ to $s=\frac{1}{2}$ electron-hole recombination scheme. Fine splittings in the central group are due to the trigonal site symmetry with components a related to [111] centers, b to [11$\bar{1}$] centers, c to [1$\bar{1}$1] centers, and d to [$\bar{1}$11] centers (compare Fig. 9).

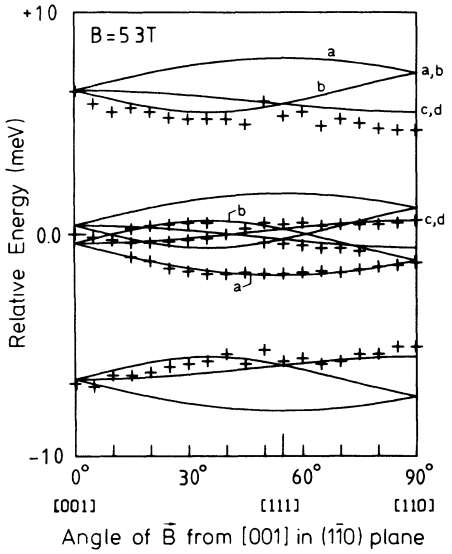

FIG. 9. Angular dependence of the (Al2)^0 Zeeman spectrum. Solid lines are fits assuming radiative recombination of an electron ($g_e=2$) with a hole ($g_{\parallel}=3.2$ and $g_{\perp}=1.6$) at a defect of trigonal (C_{3v}) site symmetry.

IV. DISCUSSION

In a previous paper[11] we noted briefly a possible relationship between the T defect (studied in some detail in that work) and the Ga1 and All centers. The data given here on All in comparison to the existing data on Ga1 (Ref. 12) and T (Ref. 11), in fact, promote this idea. Doping considerations were mainly used previously to argue that the T defect incorporates carbon and boron. Carbon incorporation was independently confirmed by a ^{13}C-^{12}C isotope shift of the NP transition. Likewise, the Ga1 center incorporates carbon and gallium, as was proved by doping studies and a carbon isotope effect on the NP line. For All the early data of Noonan *et al.*[15] and the present study demonstrate the role of aluminum in the formation of the optical center. In addition, carbon is likely involved as discussed above. Summarizing these data there is some evidence that the three defects under discussion form upon interaction of the group-III impurities boron, aluminum, or gallium with carbon. Defect constituents other than these are not obvious in the present stage of knowledge.

A strong link between the three defects is established by their common rhombic I (C_2v) site symmetry. This point group is rare for luminescent defects in irradiated

silicon, the only examples known by now being Ga1,[12,21] T,[11] and Al1 apart form Ga2, which was also assigned C_{2v} symmetry and which is related to Ga1 (Ref. 13) as a possible sucessor defect. In the three cases under discussion the symmetry assignment is based on uniaxial-stress data. For Ga1 and T it is independently arrived at by Zeeman spectroscopy which shows in addition that in both cases the luminescence is due to the radiative recombination of an isotropic electron with a noninteracting anisotropic spinlike hole. The latter statement can also be made for Al1 from the Zeeman data described in this paper. Among the three defects discussed, the quenching of the hole orbital momentum is most complete for Al1.

Common among the three defects is also their vibronic spectrum which, as the sole important feature, exhibits a mode in the 60-meV range. The vibronic satellite line is very narrow and strong in all three cases compared to true lattice modes; hence it is characteristic of the defects.

The common features mentioned here suggest that the Ga1, T, and Al1 defects have identical microscopic structure apart from the chemical difference of the group-III impurity. Significant differences exist in the annealing behavior where the luminescence from Ga1 is strong after a few days of room-temperature storage and can be slightly increased by annealing, at 150–200 °; the T-line peaks in the 400 °C range and the Al1 line at around 300 °C. Such a comparison may be of limited value for defects incorporating different impurities: The annealing behavior does not only reflect their stability, but also depends on the availability of their atomic constituents, subject to competitive defect formation and release from other defects. Evidence for such competition between Al1 and the 0.79-eV center or Ga1 and the 0.97-eV center was given for instance in the work by Noonan *et al.*[15]

For a discussion of the microscopic structure the data on Ga1 appear to be the most detailed and specific ones, but yet have not led to an unambiguous model. The simplest model consistent with the existing data and discussed previously[13,21] is a gallium-carbon pair sharing a substitutional site with its axis along a ⟨001⟩ direction. As the number of Ga and C atoms per center is not known for sure various other models appear possible. Correlation of Al1 with Al-defects as studied by EPR ($G9$, $G18$–$G21$) (Ref. 22) is unclear. Si-$G21$ could be considered the only corresponding EPR candidate as it emerges after annealing temperatures >200 °C, pairs off with another (yet unknown) defect, and was assigned monoclinic symmetry. The latter feature is inconsistent with the Al1 rhombic site symmetry; however, reorientation upon change of charge between the EPR- or PL-active states could possibly explain this discrepancy.

The second PL defect studied here, Al2, exhibits trigonal symmetry in Zeeman measurements and monoclinic symmetry in stress measurements. As discussed above, this can be explained in a dynamic model with C_{1h} being the true symmetry of the defect configuration. Aluminum incorporation in Al2 is unambiguous from the previous[15] and the present study. Based on these data, correspondence to Al_s-Al_i pairs as studied in EPR (Ref. 22) could be possible. Two pair defects, G19 and G20, were observed in the paramagnetic resonance studies with different g values and A parameters.[22] The annealing behavior of the EPR Al pairs[23] is strikingly identical to that of the Al2 defect. Moreover, the PL intensity of the Al2 spectrum is always significantly lower than for Al1 expected from a competition between the two defects when Al2 needs two aluminum atoms to form. Though these data may suggest a relationship between Al2 and the Al_s-Al_i pairs, further discussion of this point has to await more experimental data.

In conclusion, we have studied the Al1 (0.836 eV) defect luminescence spectrum and reported a new spectrum Al2 (0.886 eV) which is related to Al as well. The data on Al1 suggest that this defect is very similar or equivalent in structure to the Ga1 defect, with Al replacing the Ga, and to the T defect possibly with B as the group-III impurity. The Al2 defect shows some correspondence to Al_s-Al_i pairs as reported by EPR measurements. However, a definite correlation cannot be made at present.

Note added in proof. Recent measurements on 100% ^{13}C abundant float-zone silicon which is Al implanted and annealed at 300 °C reveal a ^{13}C-^{12}C isotope shift of the $(Al1)^0$ line of order 0.03 meV proving the incorporation of carbon in the Al1 defect.

ACKNOWLEDGMENTS

We thank W. Zulehner of Wacker Chemitronic (Burghausen) for the starting crystals. K. W. Hoffmann (Institut für Strahlenphysik, Universität Stuttgart) and E. Schäfer (Institut für Theoretische und Angewandte Physik, Universität Stuttgart) provided the irradiation facilities, and L. Raschke and G. Steudle performed the irradiation. The financial support of the Deutsche Forschungsgemeinschaft is gratefully acknowledged.

*Present address: Messerschmitt-Bölkow-Blohm, Kirchheim, Federal Republic of Germany.

†Present address: ANT Nachrichtentechnik, Backnang, Federal Republic of Germany.

‡Present address: Physikalisches Institut II, Universität Stuttgart, D-7000 Stuttgart 80, Federal Republic of Germany.

[1]For a comprehensive listing of defect photoluminescence spectra in silicon and their properties see R. Sauer, in *Impurities and Defects in Group IV and Group III–V Semiconductors*, Vol. 22b of *Landolt-Börnstein, Numerical Data and Functional Relationships in Science and Technology*, edited by K. H. Hellwege (Springer, Berlin, in press).

[2]A. V. Yukhnevich, Fiz. Tverd. Tela (Leningrad) **7**, 322 (1965), [Sov. Phys.—Solid State **7**, 259 (1965)].

[3]A. V. Yukhnevich, V. D. Tkachev, and M. V. Bortnik, Fiz. Tverd. Tela (Leningrad) **8**, 1264 (1966) [Sov. Phys.—Solid State **8**, 1004 (1966)].

[4]G. Davies and M. C. do Carmo, J. Phys. C **14**, L687 (1981).
[5]K. Thonke, H. Klemisch, J. Weber, and R. Sauer, Phys. Rev. B **24**, 5874 (1981).
[6]K. Thonke, G. D. Watkins, and R. Sauer, Solid State Commun. **51**, 127 (1984).
[7]G. Davies, E. C. Lightowlers, R. Woolley, R. Newman, and A. Oates, J. Phys. C **17**, L499 (1984).
[8]K. D. O'Donnell, K. M. Lee, and G. D. Watkins, Physica **116B**, 258 (1983).
[9]J. M. Trombetta and G. D. Watkins, Appl. Phys. Lett. **51**, 1103 (1987).
[10]K. Thonke, J. Weber, J. Wagner, and R. Sauer, Physica **116B**, 252 (1983).
[11]E. Irion, N. Bürger, K. Thonke, and R. Sauer, J. Phys. C **18**, 5069 (1985).
[12]K. Thonke, N. Bürger, and R. Sauer, Phys. Rev. B **32**, 6720 (1985), and further references therein.
[13]U. Schall, K. Thonke, and R. Sauer, Phys. Status Solidi B **137**, 305 (1986), and references therein.
[14]K. Thonke, U. Schall, and R. Sauer, Phys. Status Solidi B **137**, 291 (1986).
[15]J. R. Noonan, C. G. Kirkpatrick, and B. G. Streetman, Solid State Commun. **15**, 1055 (1974).
[16]A. Drakeford and E. C. Lightowlers, in *Materials Research Society Symposium Proceedings* (MRS, Pittsburgh, 1988), Vol. 104, p. 209.
[17]The measurements were performed by J. Wagner at the Max-Planck-Institut für Festkörperforschung, Stuttgart.
[18]A. A. Kaplyanskii, Opt. Spektrosk. **16**, 602 (1964) [Opt. Spectrosc. (USSR) **16**, 329 (1964)]; the labeling π or σ oscillator was erroneously interchanged in this reference for the rhombic I point group and has been corrected in the present paper.
[19]A. M. Stoneham, *Theory of Defects in Solids* (Clarendon, Oxford, 1975), p. 414.
[20]G. F. Koster, J. O. Dimmock, R. G. Wheeler, and H. Statz, *Properties of the Thirty-two Point Groups* (MIT, Cambridge, 1963).
[21]P. Clifton, G. Davies, and E. C. Lightowlers, J. Phys. C **17**, L889 (1984).
[22]G. D. Watkins, in *Radiation Damage in Semiconductors,* edited by P. Baruch (Dunod, Paris, 1964).
[23]G. D. Watkins, IEEE Trans. Nucl. Sci. **NS-16**, 13 (1969).